Chiral Ions in the Gas Phase, Part 6[+]

Wagner–Meerwein Rearrangements in the Gas Phase: Anchimeric Assistance to Acid-Induced Dissociation of Optically Active Phenylpropanols

Maurizio Speranza* and Antonello Filippi[a]

Abstract: The kinetics and the stereochemistry of Wagner–Meerwein rearrangements of O-protonated and O-methylated (*S*)-1-phenyl-2-propanol (**1s**$_{A^+}$; A = H or Me) and (*S*)-2-phenyl-1-propanol (**2s**$_{A^+}$; A = H or Me) have been investigated in the gas phase at 750 Torr and in the 25–140 °C temperature range. The **1s**$_{A^+}$ and **2s**$_{A^+}$ intermediates were generated in the gas phase by reaction of the $C_nH_5^+$(n = 1, 2; A = H) and $(CH_3)_2F^+$ ions (A = Me), formed by stationary γ radiolysis of bulk CH_4 and CH_3F, respectively, with the corresponding optically active alcohols. The results are consistent with unimolecular H_2O loss from both **1s**$_{H^+}$ and **2s**$_{H^+}$; this is anchimerically assisted by all the groups adjacent to the leaving moiety. Anchimeric assistance appears much less efficient in both **1s**$_{Me^+}$ and **2s**$_{Me^+}$. Analysis of the activation parameters indicates that competing neighboring-group participation in C–O bond fission in **1s**$_{H^+}$ and **2s**$_{H^+}$ respond essentially to entropic rather than enthalpic factors. The stereochemical distribution of the reaction products allowed us to discern between backside and frontside phenyl-group participation in **1s**$_{H^+}$. The counterintuitive observation of a frontside Ph participation, with an activation energy 1.3 ± 0.5 kcal mol^{-1} lower than that of the accompanying backside assistance, is attributed to conformational factors and to the stabilizing electrostatic interactions between the phenonium ion and the leaving H_2O complex that is spatially allowed only in the frontside participation and forbidden in the backside one.

Keywords: anchimeric assistance · chirality · gas-phase chemistry · phenonium ions · stereochemistry

Introduction

Stable π-bridged alkenearenium ions **I** (Scheme 1) were first proposed in 1942 by Cram as intermediates in the solvolysis of optically active β-arylalkyl tosylates.[1, 2] This hypothesis was questioned in 1962 by Brown, who instead interpreted Cram's observations in terms of the weakly π-bridged, rapidly equilibrating open ions **II**.[3] Later on, evidence was brought forth for a continuous spectrum of intermediates in the solvolysis of β-arylalkyl systems, spanning structures from **I** through to **III**, depending upon the nature of the solvent and the degree of substitution in the precursor.[4] The same factors intervene as well in the sensitive balance between anchimeric-assisted (k_Δ), solvent-assisted (k_S), and unassisted (k_C) pathways in β-arylalkyl solvolysis.[5]

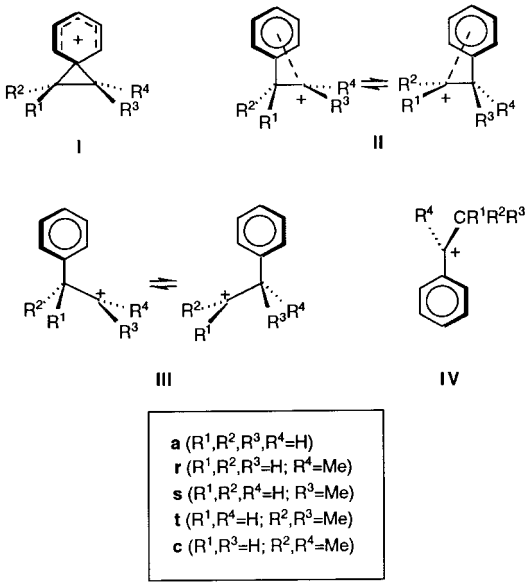

Scheme 1. Structures of phenonium ions and other isomers.

The unsubstituted phenonium ion **Ia** (Scheme 1) was directly observed by Olah and co-workers in SbF_5/SO_2ClF at

[a] Prof. M. Speranza, Dr. A. Filippi
Facoltà di Farmacia, Dipartimento No. 64
(Chimica e Tecnologia delle Sostanze Biologicamente Attive)
Università di Roma La Sapienza, P. le A. Moro 5, I-00185 Rome (Italy)
Fax: (+39) 6-49913602
E-mail: speranza@axrma.uniroma1.it

[+] Part 5: A Filippi, M. Speranza, *Int. J. Mass Spectrom. Ion Proc.*, in press.

0947-6539/99/0503-0834 $ 17.50+.50/0

$T \leq -30\,^{\circ}C$ and spectroscopically characterized as the classical spiro[5.2]octa-5,7-diene-4-ylium ion.[6, 7] Above this temperature, quantitative **Ia** → **IVa** isomerization via the open-chain structure **IIIa** was observed.[6c] In these media, however, the kinetics and mechanism of formation of **Ia** escaped determination owing to the elusive nature of its precursors. Any attempt to detect the methyl-substituted homologues of **Ia**, namely the **Is** + **Ir** racemate, in SbF_5/SO_2ClF solutions invariably failed. The only observable species were the benzyl ion **IVr** in rapid equilibrium with **IIr**.[8] Such a failure is attributable to the combined effects of side-chain substitution and of specific ion solvation that stabilize **IIIr** and **IVr**, with a large fraction of the charge adjacent to the substituent, more than **Is** + **Ir**, with most of the charge dispersed over the aromatic ring and far from the substituent. As a result, a decrease of the energy gap between **Is** + **Ir** and **IVr** is expected in the absence of solvent stabilization, together with a parallel increase of the activation barrier for their interconversion. The lower activation energy of the **Ia** → **IVa** rearrangement in superacidic media ($E^* \cong 13$ kcal mol^{-1}),[6c] relative to the estimated about 20–25 kcal mol^{-1} in the isolated state on the grounds of ab initio calculations, supports this expectation.[9]

In this context, and in view of the considerable interest in the role of ion–molecule complexes involved in gas-phase analogues of solvolysis reactions,[10] a sustained research effort was directed in the last decades to a comprehensive kinetic and mechanistic investigation about the gas-phase unimolecular dissociation of cationized β-arylalkyl systems.[11, 12] The results point to gaseous alkenearenium ions as stable intermediates that do not readily isomerize to the more stable open-chain structures **IV**.[11, 12] These open-chain isomers were found to arise from independent dissociation pathways,[11] whose extent and mechanism remain obscure. Besides, no information is presently available as to the static (**I**) or rapidly interconverting (**II**) character of the alkenearenium ions intermediates in the gas phase .

To clear up these aspects, we decided to undertake a detailed kinetic and stereochemical study of the acid-catalyzed rearrangement in some chiral β-phenyl propanols, that is (*S*)-1-phenyl-2-propanol (**1s**) and (*S*)-2-phenyl-1-propanol (**2s**), and the racemates of 1-phenyl-1-D-2-propanol (**1d**) and 2-phenyl-2-D-1-propanol (**2d**), in gaseous inert media containing an external nucleophile ($Nu^{16}OH$ or $Nu^{18}OH$; Nu = H, CH_3; Scheme 2). The kinetic approach adopted, which has

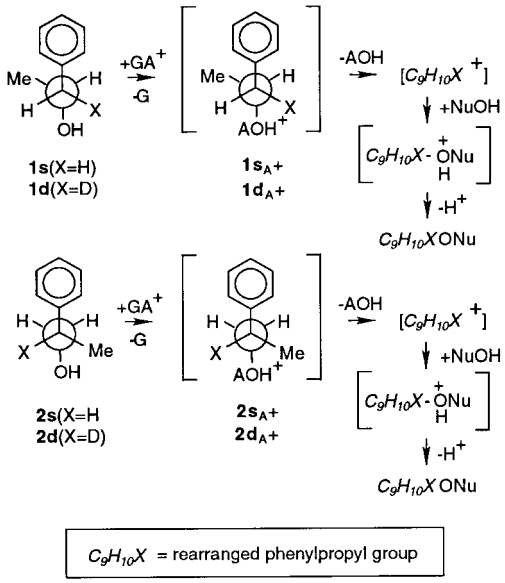

Scheme 2. Reaction patterns of O-protonated (*S*)-1-phenyl-2-propanol, 1-phenyl-1-deutero-2-propanol, (*S*)-2-phenyl-1-propanol, and 2-phenyl-2-deutero-1-propanol in the presence of methanol.

been recently reviewed,[13] is based upon the preparation of stationary concentrations of gaseous Brønsted [$GA^+ = C_nH_5^+$ ($n = 1,2$)] and Lewis acids [$GA^+ = (CH_3)_2F^+$] by γ radiolysis (^{60}Co source) of bulk gases, such as CH_4 and CH_3F (750 Torr). Attack of GA^+ on the oxygen atom of the alcoholic substrate, for example, **1s** present in traces (0.3–0.5 Torr) in the gaseous mixture, is expected to generate the corresponding oxonium ion, that is, $\mathbf{1s}_{A^+}$ (A = H or Me), wherein the loss of the leaving moiety (AOH) may be assisted by the participation of the adjacent groups.

The aim of this study is to gather more information on the gas-phase Wagner–Meerwein rearrangements in the chiral oxonium ions $\mathbf{1s}_{A^+}$ and $\mathbf{2s}_{A^+}$, and on the relevant activation parameters. It is hoped thereby to elucidate the nature of the intermediates involved in the rearrangements, as well as the role of the leaving AOH group in determining the kinetics and the dynamics of the $\mathbf{1s}_{A^+}$ and $\mathbf{2s}_{A^+}$ rearrangements.

Abstract in Italian: *La cinetica e la stereochimica del riarrangiamento di Wagner–Meerwein in (S)-1-fenil-2-propanolo (**1s**$_{A^+}$; A = H o Me) e (S)-2-fenil-1-propanolo (**2s**$_{A^+}$; A = H o Me) protonati e metilati all'atomo di ossigeno sono state studiate in fase gassosa a 750 Torr nell'intervallo di temperatura da 25 a 140 °C. Gli intermedi **1s**$_{A^+}$ e **2s**$_{A^+}$ sono stati generati in fase gassosa per attacco di ioni $C_nH_5^+$ (n = 1, 2) (A = H) e $(CH_3)_2F^+$ (A = Me), generati rispettivamente dalla γ-radiolisi stazionaria dei bulk gas CH_4 e CH_3F, sui corrispondenti alcooli enantiomericamente puri. I risultati sono in accordo con un meccanismo unimoleculare di rilascio di H_2O da **1s**$_{H^+}$ e **2s**$_{H^+}$ anchimericamente assistito da tutti i gruppi adiacenti al gruppo uscente. L'assistenza anchimerica appare molto meno efficace nel rilascio di MeOH da **1s**$_{Me^+}$ e **2s**$_{Me^+}$. L'analisi dei parametri di attivazione indica che l'assistenza anchimerica in **1s**$_{H^+}$ e **2s**$_{H^+}$ è governata da fattori entropici, piuttosto che da fattori entalpici. La distribuzione stereochimica dei prodotti di reazione da **1s**$_{H^+}$ ci permette di discernere fra l'assistenza del gruppo fenile vicinale con inversione del centro di reazione e quella che avviene con ritenzione del centro di reazione. L'osservazione controintuitiva che quest'ultimo tipo di partecipazione del Ph avvenga con una energia di attivazione minore di 1.3 ± 0.5 kcal mole^{-1} rispetto a quella riguardante la partecipazione con inversione di configurazione è attribuita a fattori conformazionali ed alle interazioni elettrostatiche stabilizzanti fra il gruppo uscente (H_2O) e la carica positiva dello ione fenonio, essenzialmente localizzata sull'anello a 6 termini. Tali interazioni sono spazialmente favorite quando la partecipazione del gruppo Ph in **1s**$_{H^+}$ avviene con ritenzione del centro di reazione.*

Table 1. Product yield and distribution from the gas-phase attack of $C_nH_5^+$ ($n = 1, 2$) and $(CH_3)_2F^+$ ions on **1s** in the presence of $Nu^{18}OH$ (Nu = H, CH_3).

Bulk gas	System composition[a] Substrate [Torr]	$Nu^{18}OH$ [Nu, Torr]	Temperature [°C]	Relative product yields [%] (^{18}O %)[b] **3s**	**3r**	**5s**	**5r**	Total absolute yield $G_{(M)}$[c]
CH_4	**1s**, 0.35	CH_3, 2.50	25	48.0(90)	7.0(90)	22.5(94)	22.5(94)	0.08 (3)
CH_4	**1s**, 0.38	CH_3, 1.54	60	60.4(93)	8.8(94)	15.3(94)	15.5(94)	0.12 (4)
CH_4	**1s**, 0.37	CH_3, 1.46	60	62.0(93)	8.0(94)	15.0(94)	15.0(94)	0.22 (8)
CH_4	**1s**, 0.47	CH_3, 1.42	100	75.7(94)	8.5(94)	8.0(94)	7.8(94)	0.20 (7)
CH_4	**1s**, 0.45	CH_3, 1.34	120	86.3(94)	7.9(94)	2.9(91)	2.9(90)	0.18 (7)
CH_4	**1s**, 0.32	CH_3, 1.40	140	89.8(93)	7.0(93)	1.6(94)	1.6(93)	0.20 (7)
CH_3F	**1s**, 0.34	H, 1.34	25	98.0(<1)	nd	1.0(36)	1.0(36)	0.47
CH_3F	**1s**, 0.38	H, 3.44	60	98.5(<1)	nd	0.7(41)	0.8(41)	0.45
CH_3F	**1s**, 0.38	H, 2.61	85	100.0(<1)	nd	nd	nd	0.48
CH_3F	**1s**, 0.44	H, 3.18	120	100.0(<1)	nd	nd	nd	0.40

[a] Bulk gas: 750 Torr; O_2: 4 Torr. Radiation dose 2×10^4 Gy (dose rate: 1×10^4 Gy h^{-1}); [b] Expressed as the percent ratio of the methylated products. Formation of alcohols **2r**, **2s**, and **1r** and ethers **4r**, **4s**, and **6** were below the detection limit (nd < 0.2 %; nd = not detected). The ^{18}O content is given in parentheses; [c] $G_{(M)}$ as the number of molecules M produced per 100 eV of absorbed energy. Each value is the average of several determinations, with an uncertainty level of approximately 5 %. The percent ratios of the overall $G_{(M)}$ values to the $G_{(GA^+)}$ of the acid precursors are given in parentheses.

Table 2. Product yield and distribution from the gas-phase attack of $C_nH_5^+$ ($n = 1, 2$) and $(CH_3)_2F^+$ ions on **2s** in the presence of $Nu^{18}OH$ (Nu = H, CH_3).

Bulk gas	System composition[a] Substrate [Torr]	$Nu^{18}OH$ [Nu, Torr]	Temperature [°C]	Relative product yields [%] (^{18}O %)[b] **1s**	**3s**	**4s**	**5s**	**5r**	**6**	Total absolute yield $G_{(M)}$ [%][c]
CH_4	**2s**, 0.41	CH_3, 1.50	25	1.3(<1)	53.6(93)	nd	16.8(93)	16.8(94)	11.5(94)	0.10 (4)
CH_4	**2s**, 0.40	CH_3, 1.63	60	4.6(<1)	72.1(94)	nd	9.8(94)	9.7(94)	3.7(94)	0.19 (7)
CH_4	**2s**, 0.41	CH_3, 1.56	85	8.4(<1)	78.8(96)	nd	5.5(96)	5.5(96)	1.8(94)	0.18 (7)
CH_4	**2s**, 0.42	CH_3, 1.61	85	7.9(<1)	78.5(95)	nd	5.8(95)	5.8(95)	2.0(94)	0.10 (4)
CH_4	**2s**, 0.51	CH_3, 1.71	120	10.4(<1)	81.5(94)	nd	3.6(94)	3.6(94)	0.9(90)	0.18 (7)
CH_3F	**2s**, 0.34	H, 2.55	25	nd	nd	100.0(<1)	nd	nd	nd	0.30
CH_3F	**2s**, 0.34	H, 3.31	60	nd	nd	100.0(<1)	nd	nd	nd	0.22
CH_3F	**2s**, 0.38	H, 2.61	85	nd	4.0(7)	96.0(<1)	nd	nd	nd	0.17
CH_3F	**2s**, 0.35	H, 2.77	140	nd	10.0(6)	90.0(<1)	nd	nd	nd	0.10

[a] Bulk gas: 750 Torr; O_2: 4 Torr. Radiation dose 2×10^4 Gy (dose rate: 1×10^4 Gy h^{-1}); [b] Expressed as the percent ratio of the products. Formation of alcohols **1r** and **2r** and ethers **3r** and **4r** were below the detection limit (nd < 0.2 %; nd = not detected). The ^{18}O content is given in parentheses; [c] see footnote [c] of Table 1.

Experimental Section

Materials: Methane, methyl fluoride, oxygen, and trimethylamine were high purity gases from Matheson, and were used without further purification. $H_2{}^{18}O$ ($^{18}O > 97$ %) and $CH_3{}^{18}OH$ ($^{18}O = 95$ %) were purchased from ICON Services. (*S*)-1-phenyl-2-propanol (**1s**) and its *R* enantiomer (**1r**), (*S*)-2-phenyl-1-propanol (**2s**) and its *R* enantiomer (**2r**), (*S*)- and (*R*)-1-phenyl-1-propanol, and 2-phenyl-2-propanol were research grade chemicals from Aldrich. The *(R,R)/(S,S)* racemate of 1-phenyl-1-deutero-2-propanol (**1d**) was synthesized, together with the *(R,S)/(S,R)* racemate of 1-phenyl-2-deutero-1-propanol, by the reaction of trans-β-methyl-styrene with $LiAlD_4$ and subsequent oxidation with hydrogen peroxide.[14] The same procedure was employed to prepare the (*R*)/(*S*)-racemate of 2-phenyl-2-deutero-1-propanol (**2d**) from α-methyl-styrene. The deuterium content of **1d** and **2d** (> 98 %) was determined by GLC–MS analysis. The methyl ethers of the above alcohols, namely, (*S*)- (**3s**) and (*R*)-1-phenyl-2-methoxypropane (**3r**), (*S*)- (**4s**) and (*R*)-2-phenyl-1-methoxypropane (**4r**), (*S*)- (**5s**) and (*R*)-1-phenyl-1-methoxypropane (**5r**), and 2-phenyl-2-methoxypropane (**6**) were synthesized by the dimethyl sulfate method, and their configuration assigned according to the starting alcohol.[15] The alcoholic substrates **1s**, **2s**, **1d**, and **2d** were purified by preparative GLC on a 2 m long, 4 mm inner diameter, stainless steel column, packed with 10 % SP-1000 on 100–120 Supelcoport, at 180 °C. Their final purity exceeded 99.95 %. The identity of the above alcohols and of their methyl ethers was verified by NMR spectroscopy and their purity assayed by GLC and GLC–MS on the same columns employed for the analysis of the irradiated mixtures.

Procedure: The gaseous mixtures were prepared by conventional techniques, with the use of a greaseless vacuum line. The reagents and the additives were introduced into carefully outgassed 130 mL Pyrex bulbs, each equipped with a break-seal tip. The bulbs were filled with the required mixture of gases, cooled to the liquid-nitrogen temperature, and sealed off. The irradiations were carried out at constant temperatures ranging from 25 to 140 °C with a ^{60}Co γ source to a dose of 2×10^4 Gy at a rate of 1×10^4 Gy h^{-1}, as determined by a neopentane dosimeter. Control experiments, carried out at doses ranging from 1×10^4 to 1×10^5 Gy, showed that the relative yields of products are largely independent of the dose. The radiolytic products were analyzed by GLC, with a Perkin–Elmer 8700 gas chromatograph equipped with a flame ionization detector, on a 25 m long, 0.25 mm inner diameter, MEGADEX DACTBS-β (30 % diacetyl-*tert*-butylsilyl-β-cyclodextrin in OV 1701) fused silica column operated at temperatures ranging from 40 to 170 °C, 4 °C min^{-1}. The products were identified by comparison of their retention volumes with those of authentic standard compounds, and their identity was confirmed by GLC–MS, with a Hewlett–Packard 5890 A gas chromatograph in line with a HP 5970 B mass spectrometer (GC–MS). Their yields were determined from the areas of the corresponding eluted peaks, with the internal standard (i.e., benzyl alcohol) method, and individual calibration factors to correct for the detector response. Blank experiments were carried out to exclude the occurrence of thermal isomerization and racemization of the starting alcohols, as well as of the corresponding methyl ethers within the temperature range investigated.

Results

Tables 1 and 2 report the absolute and relative yields of the products formed from alcohols **1s** and **2s**, respectively, undergoing gas-phase attack from the radiolytically generated GA^+ acids in the presence of O_2, as a thermal radical scavenger, and of either $H_2{}^{18}O$ or $CH_3{}^{18}OH$, as the nucleophile. The figures in the tables represent the mean percent distribution of the products, as obtained from several separate irradiations carried out under the same experimental con-

0947-6539/99/0503-0836 $ 17.50+.50/0 *Chem. Eur. J.* **1999**, *5*, No. 3

Table 3. Characteristic mass spectrometric peaks of the radiolytic products.

Radiolytic products	$^{16}O/^{18}O$-$[F]^+$	m/z	H/D-$[F]^+$	m/z
1-Phenyl-2-propanols, ***rac*-1**	$[CH_3CHOH]^+$	45 (^{16}O) 47 (^{18}O)	$[PhCH_2]^{+[c]}$	91 (H) 92 (D)
	$[PhCH_2CH(Me)OH]^{\bullet+[a]}$	136 (^{16}O) 138 (^{18}O)	$[C_7H_8]^{+[b][c]}$	92 (H) 93 (D)
			$[CH_3CHOH]^+$	45 (H) 46 (D)
2-Phenyl-1-propanols, ***rac*-2**	$[PhCH(Me)CH_2OH]^{\bullet+[a]}$	136 (^{16}O) 138 (^{18}O)	$[PhCH(Me)CH_2OH]^{\bullet+[a]}$	136 (H) 137 (D)
			$[PhCHCH_3]^{+[d]}$	105 (H) 106 (D)
1-Phenyl-2-methoxypropanes, ***rac*-3**	$[CH_3OCHCH_3]^{+[b]}$	59 (^{16}O) 61 (^{18}O)	$[PhCH_2CH(Me)OCH_3]^{\bullet+[a]}$	150 (H) 151 (D)
			$[CH_3OCHCH_3]^{+[d]}$	59 (H) 60 (D)
2-Phenyl-1-methoxypropanes, ***rac*-4**	$[PhCH(Me)CH_2OCH_3]^{\bullet+[a]}$	150 (^{16}O) 152 (^{18}O)	$[PhCH(Me)CH_2OCH_3]^{\bullet+[a]}$	150 (H) 151 (D)
	$[CH_3OCH_2]^+$	45 (^{16}O) 47 (^{18}O)	$[CH_3OCH_2]^{+[d]}$	45 (H) 46 (D)
1-Phenyl-1-methoxypropanes, ***rac*-5**	$[PhCH(OMe)CH_2CH_3]^{\bullet+[a]}$	150 (^{16}O) 152 (^{18}O)	$[PhCH(OMe)CH_2CH_3]^{\bullet+[a]}$	150 (H) 151 (D)
	$[PhCHOCH_3]^{+[b]}$	121 (^{16}O) 123 (^{18}O)	$[PhCHOCH_3]^{+[b][d]}$	121 (H) 122 (D)
2-Phenyl-2-methoxypropane, **6**	$[PhC(Me)OCH_3]^{+[b]}$	135 (^{16}O) 137 (^{18}O)	$[PhC(Me)OCH_3]^{+[b][d]}$	135 (H) 136 (D)

[a] Molecular ion. [b] Base peak. [c] Deconvolution of the m/z = 91 – 93 triplet allows determination of the extent of deuteration at the C1 center of the product. [d] The heavier fragment from the heavier molecular ion denotes location of the label at its C center. The lighter fragment from the heavier molecular ion denotes location of the label at the other C center.

ditions, and whose reproducibility is expressed by the uncertainty level quoted. The absolute yields of products are expressed as the number of molecules of the product M formed per 100 eV of energy absorbed by the gaseous mixture ($G_{(M)}$ values). The percent ratios of the overall $G_{(M)}$ values to the $G_{(GA^+)}$ of their gaseous acid precursor are quoted in parentheses.[16] The ionic character of these reactions is demonstrated by the sharp decrease of the overall product yields (over 80 %) caused by the addition to the gaseous mixture of 0.5 mol % of NMe_3, an efficient positive ion interceptor.

The presence of the ^{18}O label in the radiolytic products reported in Tables 1 and 2 is determined from 70 eV mass spectra. The ^{18}O content is measured from the intensity of the signals of their molecular ion, when present, and of the O-containing fragments (henceforth both denoted as $[F]^+$). The $[F]^+$ peaks used for evaluating the extent of ^{18}O-labelling of the radiolytic products are listed in the first half of Table 3. Since the mass spectra of the unlabeled products in Table 3 do not display any detectable signals at masses 2 amu above that of $[F]^+$ (i.e., $[F+2]^+$) the percent of ^{18}O incorporation into the products is simply calculated from the corresponding $100 \times [F+2]^+/([F]^+ + [F+2]^+)$ ratio. The relevant ^{18}O-incorporation values are reported in Tables 1 and 2 in parentheses.

Inspection of Tables 1 and 2 reveals that, in the $CH_3F/H_2{}^{18}O$ mixtures, the predominant product is always the unlabeled methyl ether of the starting alcohol (^{18}O content < 1 %), sometimes accompanied by very minor amounts of other isomers. At temperatures ≤ 60 °C, ether **3s** is obtained from the starting alcohol **1s** together with ≤ 2 % of the racemate of 1-phenyl-1-methoxypropane (***rac*-5**; ^{18}O-content = 36 – 41 %; Table 1). In contrast, at temperatures ≥ 85 °C, ether **4s** is formed from **2s** together with ≤ 10 % of (*S*)-1-phenyl-2-methoxypropane (**3s**; ^{18}O content < 7 %; Table 2).

More complex product patterns arise from the irradiated $CH_4/CH_3{}^{18}OH$ systems. Thus, abundant formation of the ^{18}O-methylated substrate (**3s**; ^{18}O content > 90 %) is observed from the starting alcohol **1s**, accompanied by minor amounts of its enantiomer (**3r**; 7.0 – 8.8 %) and of the racemate of 1-phenyl-1-methoxypropane (***rac*-5**; 3.2 – 45.0 %; Table 1). The relative distribution of these products depends upon the reaction temperature. In fact, both the [**3s**]/[**3r**] and the [**3s**]/[***rac*-5**] yield ratios are found to increase from ≈ 7 to ≈ 13 and from ≈ 1 to ≈ 28, respectively, by increasing the temperature from 25 to 140 °C.

The ^{18}O-labeled ether **3s** (^{18}O content > 93 %) predominates (53.6 – 81.5 %) among the products from the irradiated systems with **2s** (Table 2). In this case, the *R* enantiomer **3r** is never observed despite an accurate search. Instead, ether **3s** is always accompanied by minor amounts of 2-phenyl-2-methoxypropane **6** (0.9 – 11.5 %), of the racemate of 1-phenyl-1-methoxypropane ***rac*-5** (7.2 – 33.6 %), and of (*S*)-1-phenyl-2-propanol **1s** (1.3 – 10.4 %). Also in this case, the product distribution depends upon the reaction temperature, with the [**3s**]/[***rac*-5**] and [**3s**]/[**6**] yield ratios significantly increasing from 1.6 to 11.3 and from 4.7 to approximately 90.5, respectively, by increasing the temperature from 25 to 120 °C. In contrast, the [**3s**]/[**1s**] yield ratios decrease from 41.2 to 7.8 by the same temperature increase.

Ancillary experiments were carried out to gain information on the origin of the inverted (*S*)-1-phenyl-2-propanol (**1s**) recovered among the products from (*S*)-2-phenyl-1-propanol (**2s**; Table 2). Thus, mixtures containing **2s** in bulk CH_4 were irradiated at room temperature in the presence of added $H_2{}^{18}O$, as the external nucleophile. The significant incorporation of the ^{18}O label in the **1s** product (≤ 40 %) points to a prevailing acid-induced **2s** → **1s** intermolecular isomerization pathway involving uptake of the external $H_2{}^{18}O$.[17] The $[F]^+$ peaks used for evaluating the extent and the specific position of the deuterium label in the 1-phenyl-1-methoxypropanes ***rac*-5**, obtained from gas-phase protonation of the 1-phenyl-1-deutero-2-propanol (**1d**) and 2-phenyl-2-deutero-1-propanol (**2d**) racemates, are shown in the second half of Table 3. Unlabeled ***rac*-5** and their D-labeled counterparts, that is, 1-phenyl-1-deutero-1- and 1-phenyl-2-deutero-1-methoxypropanes, display very similar mass spectrometric patterns that exclude any significant isotope effect on their fragmentation. On these grounds, the D content in these products has been calculated from the molecular ion and the $[CH_3OCHCH_3]^+$ peak intensities after correction for the natural isotopic contributions. The relevant results are reported in Table 4.

Analysis of Table 4 indicates that the 1-phenyl-1-methoxypropanes ***rac*-5** formed from **1d** and **2d** retain most of the D

Table 4. Extent and position of labelling in the ***rac*-5** from deuterated starting alcohols **1d** and **2d**.[a]

Substrate [Torr]	Temperature [°C]	Nucleophile $CH_3{}^{16}OH$ [Torr]	Deuterated products [%][b] **2-D-*rac*-5**	**1-D-*rac*-5**	D content [%]
1d, 0.25	25	1.27	41.8	58.2	87
2d, 0.27	25	1.23	40.0	60.0	98
2d, 0.28	60	1.06	44.6	55.4	98
2d, 0.26	85	1.03	50.5	49.5	93
2d, 0.29	120	1.25	59.9	40.1	96

[a] Bulk gas: 750 Torr; O_2: 4 Torr. Radiation dose 2×10^4 Gy (dose rate: 1×10^4 Gy h^{-1}). Each value is the average of several determinations, with an uncertainty level of ca.10%; [b] **2-D-*rac*-5** denotes the mixture of the two racemates of diastereomeric 1-phenyl-2-deutero-1-methoxypropanes; **1-D-*rac*-5** denotes the racemate of 1-phenyl-1-deutero-1-methoxypropane.

label present in the starting alcohol, thus, ruling out any significant D exchange with the gaseous reaction medium within the 25–120 °C temperature range. Labeled ***rac*-5** exhibit the deuterium label at both C1 (**1-D-*rac*-5**) and C2 centers (**2-D-*rac*-5**). While this is not unexpected when arising from **1d**, the formation of 1-phenyl-2-deutero-1-methoxypropane (**2-D-*rac*-5**) from **2d**, in yields comparable with those of 1-phenyl-1-deutero-1-methoxypropane (**1-D-*rac*-5**) and sensitive to the reaction temperature, is rather surprising.

Discussion

Gas-phase GA^+ attack on the alcoholic substrates: The very low concentrations of alcohols **1s** and **2s** (<0.1 mol%) and of the nucleophile (0.2–0.5 mol%) present in the gaseous mixtures exclude their direct radiolysis as a significant route to the products listed in Tables 1 and 2. Addition of an efficient thermal radical scavenger (i.e., O_2) in about tenfold excess over the substrate inhibits possible free-radical reaction pathways in favor of the ionic ones, whose large predominance is testified by the marked effect of an ion trap, such as NMe_3, on the overall product yield. The trace concentration of the added nucleophile implies that all the ionic species generated from the attack of the GA^+ acids on the substrates must undergo many unreactive collisions with the bulk gas and, therefore, be thermalized prior to reaction with the neutral species present.

γ Radiolysis of the bulk gas, either CH_4 or CH_3F, generates known yields of the $C_nH_5^+$ ($n=1$, 2) and $(CH_3)_2F^+$ acids, respectively. Once collisionally thermalized, these ions efficiently attack all the nucleophiles present in the mixture, including $H_2{}^{16}O$, which is a ubiquitous impurity present in the irradiated systems. As a consequence, in the CH_4/**1s** (or **2s**)/$CH_3{}^{18}OH$ mixtures, the initially formed $C_nH_5^+$ ($n=1$, 2) Brønsted acids can attack either the alcoholic substrate, yielding inter alia the corresponding O-protonated derivative [henceforth denoted as $\mathbf{1s}_{H^+}$ (or $\mathbf{2s}_{H^+}$)], and the added $CH_3{}^{18}OH$ (or the ubiquitous $H_2{}^{16}O$ impurity), yielding eventually the $CH_3{}^{18}OH_2^+$ Brønsted acid. Similarly, in the CH_3F/**1s** (or **2s**)/$H_2{}^{18}O$ systems, the initially formed $(CH_3)_2F^+$ Lewis acid can attack either the alcoholic substrate, yielding the corresponding O-methylated derivative [henceforth denoted as $\mathbf{1s}_{Me^+}$ (or $\mathbf{2s}_{Me^+}$)], or the added $H_2{}^{18}O$ (and the ubiquitous $H_2{}^{16}O$ isotopomer), giving rise to the corresponding $CH_3{}^{18}OH_2^+/CH_3{}^{16}OH_2^+$ pair, in proportions depending upon the $[H_2{}^{18}O]/[H_2{}^{16}O]$ ratio. Therefore, the nature and the relative distribution of the acidic species, generated in the irradiated samples, are determined by the nature of the bulk gas and by presence and the relative concentration of the nucleophiles present in the mixture. All these acidic species can eventually attack the selected substrates, provided that the process is thermochemically allowed.

The evaluation of the thermochemistry of the reaction sequences of Scheme 2 meets with some difficulty owing to the lack of experimental thermochemical data for the involved ionic species, for example, $\mathbf{1s}_{H^+}$ (or $\mathbf{2s}_{H^+}$) and $\mathbf{1s}_{Me^+}$ (or $\mathbf{2s}_{Me^+}$), and neutral substrates, that is, **1s** and **2s**. However, approximate values of the relevant reaction enthalpies can be inferred from the thermochemical data reported in Table 5,

Table 5. Thermochemical data [kcal mol^{-1}; estimated values in italics].

Species	ΔH_f°	Species	ΔH_f°
CH_4	−17.8[a]	**1s**	*−33*[b]
C_2H_4	12.5[a]	**2s**	*−33*[b]
H_2O	−58[a]	$\mathbf{1s}_{H^+}$	*136*[c]
CH_3OH	−48[a]	$\mathbf{2s}_{H^+}$	*139*[c]
CH_3F	−59[a]	$\mathbf{1s}_{Me^+}$	*130*[d]
CH_5^+	216[a]	$\mathbf{2s}_{Me^+}$	*133*[d]
$C_2H_5^+$	215.6[a]	**Ir**	*199*[e]
$(CH_3)_2F^+$	147[a]	**IVr**	186[a]
$CH_3OH_2^+$	136[a]	**IVs**	*191*[f]

[a] S. G. Lias, J. E. Bartmess, J. F. Liebman, J. L. Holmes, R. D. Levin, W. G. Mallard, *J. Phys. Chem. Ref. Data* **1988**, *17*, Suppl. 1. [b] Estimated by the group additivity method (S. W. Benson, *Thermochemical Kinetics*, Wiley, New York, **1968**. [c] Estimated from the proton affinity (PA) limits of primary and secondary alcohols (194 and 197 kcal mol^{-1}, respectively); J. Long, B. Munson, *J. Am. Chem. Soc.* **1973**, *95*, 2427. [d] Estimated by $\Delta PA = PA(\text{methyl ether}) - PA(\text{alcohol}) = 10$ kcal mol^{-1} (R. D. Bowen, D. H. Williams, *J. Am. Chem. Soc.* **1978**, *100*, 7545; R. D. Bowen, D. H. Williams, G. Hvistendahl, J. R. Kalman, *Org. Mass Spectrom.* **1978**, *13*, 721). The heats of formation of the neutral methyl ethers have been calculated as in footnote [b]. [e] Estimated by correcting the enthalpy of formation of **Ia** (204 kcal mol^{-1}; M. Mishima, Y. Tsuno, M. Fujio, *Chem. Lett.* **1990**, 2277) for the stabilizing effect of the methyl substituent on the cyclopropyl ring, taken as equal to that on the cyclopropylcarbinyl cation (≈5 kcal mol^{-1}; W. J. Hehre, P. Hiberty, *J. Am. Chem. Soc.* **1974**, *96*, 302). [f] Estimated by correcting the enthalpy of formation of α-phenylethyl cation (199 kcal mol^{-1}; ref. [a]) for the stabilizing effect of the methyl substituent at the C_β (≈1 kcal mol^{-1}).

some of which were derived from the well-established estimation procedures outlined in the footnotes of the table. From the relevant ΔH_f° values, the first steps of Scheme 2 with $GA^+ = C_nH_5^+$ ($n=1$, 2), $CH_3OH_2^+$, and $(CH_3)_2F^+$ are all thermochemically allowed [$-\Delta H^\circ = 12-65$ kcal mol^{-1}; Eqs. (1)–(8) in Table 6].

Unimolecular C–O bond cleavage in the primary oxonium intermediates $\mathbf{1s}_{H^+}$ (or $\mathbf{2s}_{H^+}$) to give either **IVr** or **IVs** is thermochemically allowed as well [$-\Delta H^\circ = 3-11$ kcal mol^{-1}; Eqs. (10), (11), (13), and (14) in Table 6], whereas the hypothetical one yielding separated **Ir** and H_2O is slightly endothermic [$\Delta H^\circ = 2-5$ kcal mol^{-1}; Eqs. (9) and (12) in Table 6]. Nevertheless, taking into account the favorable entropic factors, this latter process can also be regarded as thermodynamically accessible. Another factor, particularly relevant in gaseous systems at high pressures, concerns the possibility that C–O bond cleavage in the oxonium inter-

0947-6539/99/0503-0838 $ 17.50+.50/0 *Chem. Eur. J.* **1999**, *5*, No. 3

Table 6. Reaction enthalpies [kcal mol^{-1}].

	Neutral reactant		Ionic reactant		Reaction products			ΔH°
1	**1s**	+	CH_5^+	→	$\mathbf{1s}_{H^+}$	+	CH_4	−65
2	**1s**	+	$C_2H_5^+$	→	$\mathbf{1s}_{H^+}$	+	C_2H_4	−34
3	**1s**	+	$CH_3OH_2^+$	→	$\mathbf{1s}_{H^+}$	+	CH_3OH	−15
4	**1s**	+	$(CH_3)_2F^+$	→	$\mathbf{1s}_{Me^+}$	+	CH_3F	−43
5	**2s**	+	CH_5^+	→	$\mathbf{2s}_{H^+}$	+	CH_4	−62
6	**2s**	+	$C_2H_5^+$	→	$\mathbf{2s}_{H^+}$	+	C_2H_4	−31
7	**2s**	+	$CH_3OH_2^+$	→	$\mathbf{2s}_{H^+}$	+	CH_3OH	−12
8	**2s**	+	$(CH_3)_2F^+$	→	$\mathbf{2s}_{Me^+}$	+	CH_3F	−40
9			$\mathbf{1s}_{H^+}$	→	**Ir**	+	H_2O	+5
10			$\mathbf{1s}_{H^+}$	→	**IVs**	+	H_2O	−3
11			$\mathbf{1s}_{H^+}$	→	**IVr**	+	H_2O	−8
12			$\mathbf{2s}_{H^+}$	→	**Ir**	+	H_2O	+2
13			$\mathbf{2s}_{H^+}$	→	**IVs**	+	H_2O	−6
14			$\mathbf{2s}_{H^+}$	→	**IVr**	+	H_2O	−11
15			$\mathbf{1s}_{Me^+}$	→	**Ir**	+	CH_3OH	+21
16			$\mathbf{1s}_{Me^+}$	→	**IVs**	+	CH_3OH	+13
17			$\mathbf{1s}_{Me^+}$	→	**IVr**	+	CH_3OH	+8
18			$\mathbf{2s}_{Me^+}$	→	**Ir**	+	CH_3OH	+18
19			$\mathbf{2s}_{Me^+}$	→	**IVs**	+	CH_3OH	+10
20			$\mathbf{2s}_{Me^+}$	→	**IVr**	+	CH_3OH	+5
21	CH_3OH	+	$\mathbf{1s}_{H^+}$	→	$\mathbf{1r}_{Me^+}$	+	H_2O	−16
22	CH_3OH	+	$\mathbf{2s}_{H^+}$	→	$\mathbf{2s}_{Me^+}$	+	H_2O	−16

mediates gives rise to stable, electrostatically bonded adducts between the $C_9H_{11}^+$ and AOH fragments. In this way, the enthalpy of $\mathbf{1s}_{H^+}$ (or $\mathbf{2s}_{H^+}$) dissociation is lowered by a quantity corresponding to the $[C_9H_{11}^+ \cdot H_2O]$ binding energy (easily exceeding 10 kcal mol^{-1}).[18] In this case, fragmentation of $\mathbf{1s}_{H^+}$ (or $\mathbf{2s}_{H^+}$) into the $[\mathbf{Ir} \cdot H_2O]$ complex becomes energetically accessible. The same considerations apply to the unimolecular C–O bond cleavage in $\mathbf{1s}_{Me^+}$ (or $\mathbf{2s}_{Me^+}$) [Eqs. (15) – (20) in Table 6]. Here, unimolecular conversion of $\mathbf{1s}_{Me^+}$ (or $\mathbf{2s}_{Me^+}$) into the $[\mathbf{IVr} \cdot CH_3OH]$ and $[\mathbf{IVs} \cdot CH_3OH]$ complexes are energetically feasible [Eqs. (16), (17), (19), and (20) in Table 6],[18] whereas the $\mathbf{1s}_{Me^+}$ (or $\mathbf{2s}_{Me^+}$) → $[\mathbf{Ir} \cdot CH_3OH]$ one appears thermodynamically forbidden [Eqs. (15) and (18) in Table 6]. A CH_3OH-to-H_2O bimolecular pathway can be also conceived to account for the formation of the ethereal products in Tables 1 and 2 [$-\Delta H^\circ = 16$ kcal mol^{-1}; Eqs. (21) and (22) in Table 6].

Besides the oxygen atom, another basic site is present in the selected substrates, namely, the phenyl ring, which may compete with the oxygen center for the gaseous GA^+ acids. For the purposes of the present work, ring protonation of the aromatic substrate by Brønsted GA^+ acids is a parasitic, unproductive process. Occurrence of this blind reaction may account for the limited absolute yields of the ethereal products reported in Tables 1 and 2. Another conceivable reason resides in the diverse aptitude of the various Brønsted GA^+ acids, formed in the irradiated mixtures, to promote the reaction patterns of Scheme 2. Indeed, in agreement with previous evidence,[11] the $CH_3{}^{18}OH_2^+$ Brønsted acid, which is abundantly generated in both the CH_4 and CH_3F mixtures, appears to be rather ineffective in catalyzing any substrate rearrangement, although able to O-protonate **1s** (or **2s**) [Eqs. (3) and (7) in Table 6]. A clear symptom of its inefficiency is provided by the exceedingly low amounts of the ^{18}O-labeled products ($\leq 0.7\,\%$) formed in the CH_3F/**1s**/$H_2{}^{18}O$ (Table 1) and CH_3F/**2s**/$H_2{}^{18}O$ systems at any temperature (Table 2). This excludes occurrence of the intracomplex mechanism of Scheme 3 to any significant extent. A rationale for such an inefficiency can be found in the likely formation of a stable proton-bonded adduct **V**, whose rearrangement or fragmentation before neutralization appears to be inhibited at 750 Torr by the rapid collisional quenching with the bulk gas

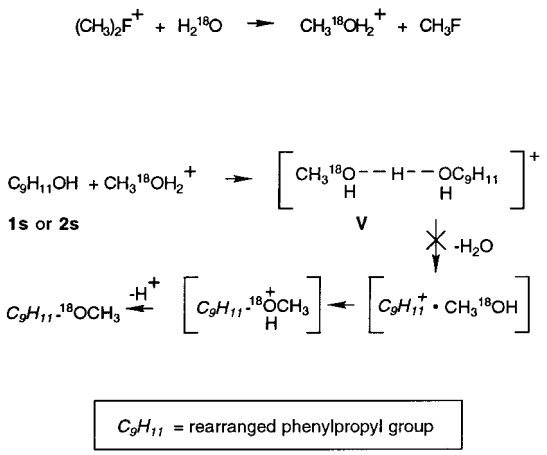

Scheme 3. Hypothetical $CH_3{}^{18}OH_2^+$-catalyzed intracomplex displacement reaction.

molecules. On these grounds, it can be concluded that the acid catalysts active in the $CH_4/CH_3{}^{18}OH$ and $CH_3F/H_2{}^{18}O$ mixtures are the $C_nH_5^+$ ($n = 1$, 2) and the $(CH_3)_2F^+$ ions, respectively.

In this context, assuming equal the collision frequencies between the radiolytic $C_nH_5^+$ ($n = 1$, 2) ions and the neutral nucleophiles present in the $CH_4/CH_3{}^{18}OH$ systems, that is, $CH_3{}^{18}OH$, $H_2{}^{16}O$, and the alcoholic substrate **1s** (or **2s**), the theoretical overall absolute yield of products can be approximately expressed by $\{G(C_nH_5^+(n=1,2)) \times [\mathbf{1s}\ (\text{or}\ \mathbf{2s})]\}/\{[CH_3{}^{18}OH] + [H_2{}^{16}O] + [\mathbf{1s}\ (\text{or}\ \mathbf{2s})]\} = 0.2 - 0.3$.[16, 17] Thus, the closeness of these estimates with the $G_{(M)}$ values given in Tables 1 and 2 indicates that trapping of the $\mathbf{1s}_{H^+}$ (or $\mathbf{2s}_{H^+}$) intermediates (and of their derivatives) by $CH_3{}^{18}OH$ is a very efficient process.

The reaction pattern: The almost exclusive recovery of unlabeled **3s** from the CH_3F/**1s**/$H_2{}^{18}O$ mixtures and of unlabeled **4s** from CH_3F/**2s**/$H_2{}^{18}O$ clearly demonstrates that the $\mathbf{1s}_{Me^+}$ and $\mathbf{2s}_{Me^+}$ intermediates, once formed from the attack of $(CH_3)_2F^+$ at the oxygen atom of **1s** and **2s**, are very stable gaseous species with no propensity towards rearrangement or fragmentation. Only in the CH_3F/**2s**/$H_2{}^{18}O$ systems at the highest temperatures ($T \geq 85\,^\circ C$; Table 2), it is possible to observe the formation of small amounts (4 – 10 %) of mostly unlabeled **3s**. Taking into account that its formation from **2s** requires complete inversion of configuration of the chiral center, it is suggested that the reaction proceeds through the irreversible $\mathbf{2s}_{A^+} \rightarrow [\mathbf{Ir} \cdot AOH] \rightarrow \mathbf{1s}_{A^+}$ (A = CH_3) intracomplex rearrangement followed by proton loss to a suitable base [sequence ii) → i) of Scheme 4].[19] At first glance, an analogous intracomplex process with A = H could be taken as being responsible for the formation of the unlabeled inverted **1s** product in the CH_4/**2s**/$CH_3{}^{18}OH$ systems at any temperature

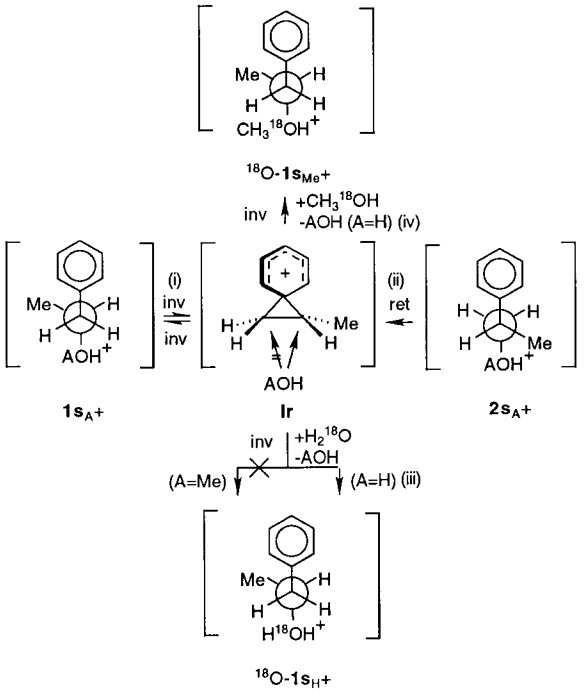

Scheme 4. Inter- and intramolecular reaction patterns.

(Table 2). However, the observation that **1s** produced in the CH_4/**2s**/$H_2{}^{18}O$ systems incorporates an appreciable amount of the ^{18}O label ($\leq 40\,\%$; see Results section) suggests that the [**Ir**·H_2O] complex may undergo extensive $H_2{}^{18}O$-to-H_2O ligand exchange [path iii) of Scheme 4].[17] The absence of labeled **1s** from the CH_3F/**2s**/$H_2{}^{18}O$ systems indicates that an analogous $H_2{}^{18}O$-to-CH_3OH ligand exchange does not take place in the [**Ir**·CH_3OH] complex prior to intracomplex covalent rebonding to **1s**$_{Me^+}$.

Ether **3s** is the major product from both the CH_4/**1s**/$CH_3{}^{18}OH$ (Table 1) and the CH_4/**2s**/$CH_3{}^{18}OH$ systems (Table 2) under all conditions. Its formation from **1s** requires retention of the configuration of the chiral center, whereas its formation from **2s** requires inversion of the configuration of the chiral center. This observation rules out any mechanism other than the unimolecular sequences i) →iv) and ii) →iv) of Scheme 4 (A = H). In fact, the conceivable S_N2 processes [Eqs. (21) and (22) in Table 6] would yield preferentially the inverted **3r** from **1s** and the retained **4s** from **2s**. Furthermore, the pronounced **3s** versus **3r** unbalance from **1s** speaks against the intermediacy of the open 1-phenyl-2-propyl cation from simple C–O bond fission in **1s**$_{H^+}$. In this case, trapping of the free 1-phenyl-2-propyl cation by the present nucleophiles would give rise eventually to the racemate of the corresponding products (e.g., ***rac*-3**), in contrast with the experimental evidence. The intermediacy of the primary 2-phenyl-1-propyl cation from simple C–O bond cleavage in **2s**$_{H^+}$ is excluded a fortiori. Therefore, in agreement with previous indications,[11] the oxonium intermediates **1s**$_{H^+}$ and **2s**$_{H^+}$ undergo fast unimolecular C–O bond fission assisted by the participation of the vicinal groups. If the participating moiety is the phenyl group, the process leads to a relatively stable phenonium ion. Irrespective of the stereochemistry of the process, the **2s** alcohol only give rise to the retained phenonium ion **Ir**. Hence, the exclusive formation of the inverted ether **3s** from **2s** points to the irreversible backside attack of the external $CH_3{}^{18}OH$ at the methyl-substituted center of **Ir**. In this context, formation of the retained ether **3s** from **1s** (48.0–89.8 %; Table 1) must proceed through the two step sequence i) →iv) of Scheme 4, each step involving inversion of the configuration of the chiral center. In view of the complete backside attack of the external $CH_3{}^{18}OH$ in step iv), formation of the inverted ether **3r** from **1s** (7.0–8.8 %; Table 1) necessarily involves retention of the configuration of the chiral center in step i) of the sequence (i.e. **1s**$_{H^+}$ →**Is** + H_2O). In other words, the **3s** versus **3r** pattern from **1s** (Table 1) reflects the competition between backside versus frontside participation of the phenyl group in the unimolecular C–O bond cleavage in **1s**$_{H^+}$ to give the corresponding 1,2-propenebenzenium enantiomers **Ir** and **Is**.

Concerning the genesis of the 1-phenyl-1-methoxypropane racemate (***rac*-5**) and 2-phenyl-2-methoxypropane (**6**) products reported in Tables 1 and 2, the question arises as to whether it involves the participation of adjacent groups other than phenyl, that is the hydrogen atom or the methyl group, in the unimolecular C–O bond fission in **1s**$_{H^+}$ and **2s**$_{H^+}$, or whether it is due to the partial unimolecular isomerization of the phenonium ion structure. Unequivocal assessment of this point is crucial for rationalizing the factors affecting the relative distribution of the ethereal products in Tables 1 and 2, and their dependence upon the reaction temperature. Several pieces of evidence rule out the latter hypothesis in favor of the first one, including:

1) The evident difference in the product patterns from **1s** (Table 1) and **2s** (Table 2) under identical experimental conditions, which is not compatible with the intermediacy of a single phenonium ion structure. Besides, the sizable yields of ***rac*-5** from **1s** and the complete absence of **6** (Table 1), which is an appreciable product from **2s** (Table 2), points to a rather inefficient **IVs** ↔ **IVr** interconversion under the conditions used.
2) The negative temperature dependence of the [***rac*-5**]/[**3r**] and [***rac*-5**]/[**3s**] from **1s** (Table 1) and of the [***rac*-5**]/[**3s**] and [**6**]/[**3s**] ratios from **2s** (Table 2). Raising the temperature would in fact favor rearrangement of the phenonium ion structure to the thermodynamically more stable ones **IVr** and **IVs** (Table 3).

On these grounds, and in agreement with previous indirect evidence,[11] we conclude that the products of Table 1 are generated by the reaction network of Scheme 5, involving competing neighboring-group participation in the unimolecular C–O bond cleavage in the **1s**$_{H^+}$ precursor.

A similar competition network (Scheme 6) accounts for the formation of the products of Table 2. Thus, alcohol **1s** and ether **3s** arise from phenyl-group participation in the unimolecular C–O bond cleavage in **2s**$_{H^+}$. This process competes with hydrogen-atom participation leading directly to ether **6**. Concerning the origin of ethers ***rac*-5**, methyl-group participation in **2s**$_{H^+}$ does not explain by itself the observations reported in Table 4. Indeed, methyl-group participation in the racemate of *O*-protonated 2-phenyl-2-deutero-1-propanol (**2d**$_{H^+}$) would generate ethers ***rac*-5** with the deuterium label exclusively located at the C1 center, that is, **1-D-*rac*-5**. The

0947-6539/99/0503-0840 $ 17.50+.50/0 *Chem. Eur. J.* **1999**, *5*, No. 3

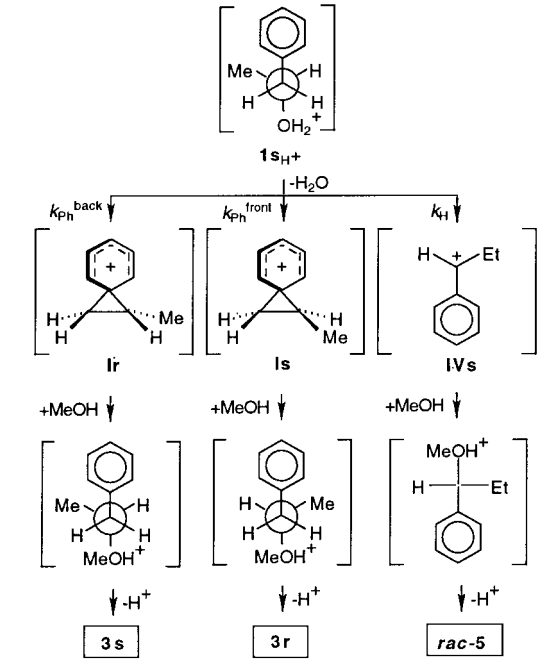

Scheme 5. Reaction pattern from gas-phase O-protonation of (*S*)-1-phenyl-2-propanol in the presence of methanol.

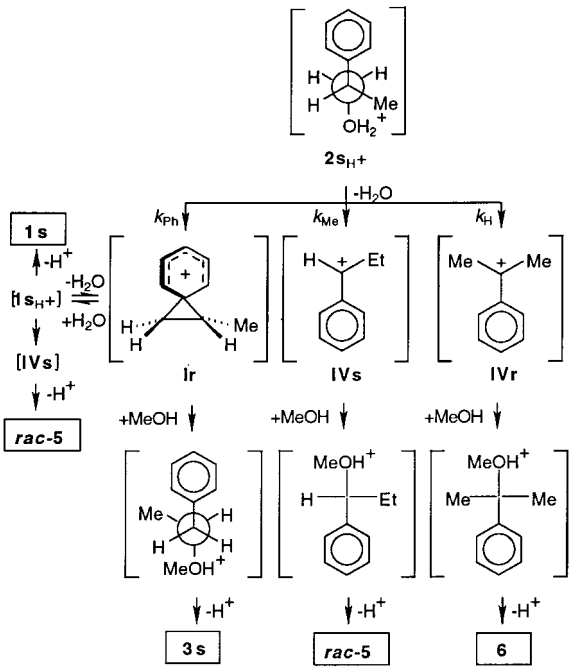

Scheme 6. Reaction pattern from gas-phase O-protonation of (*S*)-2-phenyl-1-propanol in the presence of methanol.

observation that these labeled ethers are accompanied by those with the deuterium label at the C2 center (i.e., **2-D-*rac*-5**) points to an additional route to ethers ***rac*-5** from **2d**$_{H^+}$. The position of the label in the **2-D-*rac*-5** from **2d**$_{H^+}$, coupled with the isolation of appreciable amounts of the rearranged alcohol **1s** from **2s**$_{H^+}$, suggests that formation of both these products involves the **1s**$_{H^+}$ intermediate in the sequence ii) → iii) [A = H] of Scheme 4, followed by its neutralization to **1s** in competition with the hydrogen-atom-assisted H_2O loss shown in Scheme 5 (k_H). From this, we can conclude that formation of the products of Table 2 follow the reaction network shown in Scheme 6. Accordingly, the **1-D-*rac*-5** versus **2-D-*rac*-5** relative distributions, reported in Table 4, can be taken in the first approximation as reflecting the relative contribution at any given temperature of the channels involving intermediates **IVs** and **1s**$_{H^+}$ in the formation of ethers ***rac*-5** from **2s**$_{H^+}$ (Table 2).[20]

Neighboring-group participation and anchimeric assistance: In the context of the reaction networks of Schemes 5 and 6, the relative rate constants of the competing neighboring-group participation in **1s**$_{H^+}$ and **2s**$_{H^+}$ can be simply inferred from the yield ratios of the relevant labeled ethereal products. Thus, the ratios [**3s**]/[***rac*-5**], [**3r**]/[***rac*-5**], and [**3s**]/[**3r**] from Table 1 express the k_{Ph}^{back}/k_H, k_{Ph}^{front}/k_H, and $k_{Ph}^{back}/k_{Ph}^{front}$ rate constant ratios, respectively, shown in Scheme 5. The corresponding values are reported in Table 7 and their dependence upon the reaction temperature (25 – 140 °C) is shown in Figure 1. In the same way, the {[**3s**] + [**1s**] + [**2-D-*rac*-5**]}/[**1-D-*rac*-5**] ratios from Tables 2 and 4, reflect the k_{Ph}/k_{Me} rate-constant ratio (Scheme 6), while the {[**3s**] + [**1s**] + [**2-D-*rac*-5**]}/[**6**] and [**1-D-*rac*-5**]/[**6**] ratios provide a measure of the k_{Ph}/k_H and k_{Me}/k_H rate-constant ratios, respectively. The corresponding values are listed in Table 8 and their dependence upon the reaction temperature (25 – 120 °C) is illustrated in Figure 2. The linearity of the $\log(k_{Ph}^{back}/k_{Ph}^{front})$ versus T^{-1} dependence of Figure 1 is consistent with independent backside versus frontside phenyl-group participation in C–O bond

Table 7. Rate constant ratios of intramolecular isomerization of **1s**$_{H^+}$ in CH_4 at 750 Torr.[a]

Temperature [°C]	$k_{Ph}^{back}/k_{Ph}^{front}$	k_{Ph}^{front}/k_H	k_{Ph}^{back}/k_H
25	6.86 (0.863)	0.16 (–0.808)	1.07 (0.028)
60	6.86 (0.863)	0.29 (–0.544)	1.96 (0.292)
60	7.75 (0.889)	0.27 (–0.574)	2.07 (0.315)
100	8.91 (0.950)	0.54 (–0.269)	4.79 (0.680)
120	10.92 (1.038)	1.36 (0.134)	14.88 (1.173)
140	12.83 (1.108)	2.19 (0.340)	28.06 (1.448)

[a] Each value is the average of several determinations, with an uncertainty level of ca.10%. $k_{Ph}^{back}/k_{Ph}^{front}$ = [**3s**]/[**3r**]; k_{Ph}^{front}/k_H = [**3r**]/[***rac*-5**]; k_{Ph}^{back}/k_H = [**3s**]/[***rac*-5**]. Logarithm of the ratios in parentheses.

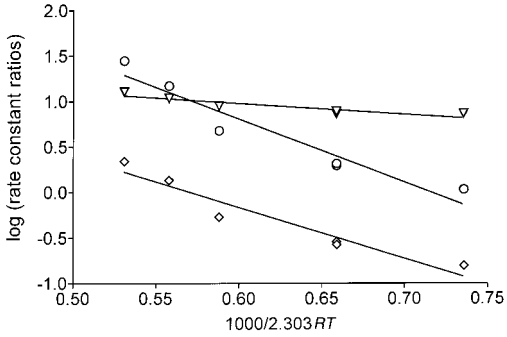

Figure 1. Arrhenius plots for the competing backside phenyl versus hydride (circles), frontside phenyl versus hydride (diamonds), and backside versus frontside phenyl participation (triangles) to the C–O bond cleavage in **1s**$_{H^+}$.

Table 8. Rate constant ratios of intramolecular isomerization of $\mathbf{2s}_{H^+}$ in CH_4 at 750 Torr.[a]

Temperature [°C]	k_{Ph}/k_{Me}	k_{Ph}/k_H	k_{Me}/k_H
25	3.39 (0.530)	5.94 (0.774)	1.75 (0.244)
60	7.90 (0.898)	23.08 (1.363)	2.92 (0.465)
85	17.03 (1.231)	51.53 (1.721)	3.02 (0.481)
85	16.07 (1.206)	46.13 (1.664)	2.87 (0.458)
120	33.32 (1.523)	106.90 (2.029)	3.21 (0.506)

[a] Each value is the average of several determinations, with an uncertainty level of ca.10%. $k_{Ph}/k_{Me} = \{[\mathbf{3s}] + [\mathbf{1s}] + [\mathbf{2\text{-}D\text{-}}\textit{rac}\text{-}\mathbf{5}]\}/[\mathbf{1\text{-}D\text{-}}\textit{rac}\text{-}\mathbf{5}]$; $k_{Ph}/k_H = \{[\mathbf{3s}] + [\mathbf{1s}] + [\mathbf{2\text{-}D\text{-}}\textit{rac}\text{-}\mathbf{5}]\}/[\mathbf{6}]$; $k_{Me}/k_H = [\mathbf{1\text{-}D\text{-}}\textit{rac}\text{-}\mathbf{5}]/[\mathbf{6}]$. Logarithm of the ratios in parentheses.

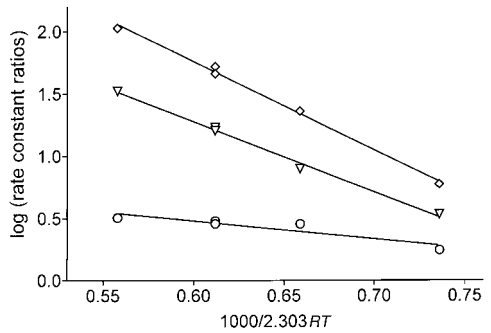

Figure 2. Arrhenius plots for the competing phenyl versus methyl (triangles), methyl versus hydride (circles), and phenyl versus hydride participation (diamonds) to the C–O bond cleavage in $\mathbf{2s}_{H^+}$.

fission in $\mathbf{1s}_{H^+}$ and excludes any significant $\mathbf{Ir} \leftrightarrow \mathbf{Is}$ interconversion even at the highest temperatures. Given the relatively long lifetime of 1,2-propenebenzenium intermediate (ca. 2×10^{-8} s),[21] corresponding to many thousands C–C bond rotations, its reluctance to rearrange or racemize unimolecularly in the gas phase corresponds to a static cyclic structure **I**, rather than to the rapidly equilibrating open ones **II** (Scheme 1).

Regression analysis of the linear curves of Figures 1 and 2 leads to the differential activation parameters listed in Table 9. The relevant absolute values can be rationalized as

Table 9. Differential Arrhenius parameters for the competing neighboring-group participation to the C–O bond cleavage in $\mathbf{1s}_{H^+}$ and $\mathbf{2s}_{H^+}$.

Competing reactions[a]	Arrhenius equation[b]	Correlation coefficient, r
$\mathbf{Ir} \leftarrow \mathbf{1s}_{H^+} \rightarrow \mathbf{IVs}$	$\log(k_{Ph}^{back}/k_H) = (5.0 \pm 0.3) - (7.0 \pm 0.3)x$	0.960
$\mathbf{Is} \leftarrow \mathbf{1s}_{H^+} \rightarrow \mathbf{IVs}$	$\log(k_{Ph}^{front}/k_H) = (3.2 \pm 0.3) - (5.6 \pm 0.3)x$	0.964
$\mathbf{Ir} \leftarrow \mathbf{1s}_{H^+} \rightarrow \mathbf{Is}$	$\log(k_{Ph}^{back}/k_{Ph}^{front}) = (1.7 \pm 0.5) - (1.3 \pm 0.5)x$	0.927
$\mathbf{Ir} \leftarrow \mathbf{2s}_{H^+} \rightarrow \mathbf{IVs}$	$\log(k_{Ph}/k_{Me}) = (4.7 \pm 0.2) - (5.7 \pm 0.2)x$	0.997
$\mathbf{Ir} \leftarrow \mathbf{2s}_{H^+} \rightarrow \mathbf{IVr}$	$\log(k_{Ph}/k_H) = (6.0 \pm 0.2) - (7.1 \pm 0.2)x$	0.997
$\mathbf{IVs} \leftarrow \mathbf{2s}_{H^+} \rightarrow \mathbf{IVr}$	$\log(k_{Me}/k_H) = (1.3 \pm 0.5) - (1.4 \pm 0.5)x$	0.906

[a] H_2O as byproduct; [b] $x = 1000/2.303RT$.

follows. In view of the inertness of the encounter complex **V** (Scheme 3) towards rearrangement and dissociation, the closeness of the $G_{(M)}$ values in Tables 1 and 2 with the maximum theoretical yields can be explained only by extensive structural rearrangement of $\mathbf{1s}_{H^+}$ and $\mathbf{2s}_{H^+}$ well before their trapping by the external $CH_3{}^{18}OH$. Therefore, timing of the neighboring-group participation in the C–O bond fission in $\mathbf{1s}_{H^+}$ and $\mathbf{2s}_{H^+}$ must fall well within the collision interval of $\mathbf{1s}_{H^+}$ (or $\mathbf{2s}_{H^+}$) with $CH_3{}^{18}OH$ ($\tau = 2 \times 10^{-8}$ s).[21] It follows that the absolute rate constant of the fastest rearrangement in $\mathbf{1s}_{H^+}$ and $\mathbf{2s}_{H^+}$, namely, that involving phenyl-group participation, should greatly exceed $1/\tau = 5 \times 10^7$ s^{-1}. On the one hand, the differential activation parameters of Table 9, in particular the $\Delta E^*(\mathbf{Ir} \leftarrow \mathbf{1s}_{H^+} \rightarrow \mathbf{IVs}) = 7.0 \pm 0.3$ kcal mol^{-1} and $\Delta E^*(\mathbf{Ir} \leftarrow \mathbf{2s}_{H^+} \rightarrow \mathbf{IVr}) = 7.1 \pm 0.3$ kcal mol^{-1}, demand that this lower rate limit should correspond to an activation energy for the phenyl-group participation $\mathbf{1s}_{H^+} \rightarrow \mathbf{Ir} \leftarrow \mathbf{2s}_{H^+}$ of at least 7–8 kcal mol^{-1}, which in turn corresponds to the negligible activation energy for the competing hydrogen participation $\mathbf{1s}_{H^+} \rightarrow \mathbf{IVs}$ and $\mathbf{2s}_{H^+} \rightarrow \mathbf{IVr}$. On the other hand, the same lower rate limit excludes activation barriers in excess of 8–10 kcal mol^{-1} for the $\mathbf{1s}_{H^+} \rightarrow \mathbf{Ir} \leftarrow \mathbf{2s}_{H^+}$ process, since otherwise the corresponding preexponential factors would exceed the maximum theoretical value of 10^{13}–10^{14} s^{-1}. On these grounds, we calculate that the absolute activation energy for the phenyl-group participation in $\mathbf{1s}_{H^+}$ and $\mathbf{2s}_{H^+}$ (E_{Ph}^*) amounts to 9 ± 2 kcal mol^{-1}. This means that the absolute activation energy for the hydride participation in $\mathbf{1s}_{H^+}$ and $\mathbf{2s}_{H^+}$ (E_H^*) is around 2 ± 2 kcal mol^{-1}, and that for the methyl-group participation in $\mathbf{2S}_{H^+}$ (E_{Me}^*) is around 4 ± 2 kcal mol^{-1}. Comparison of these activation barriers with the much larger energy required for the simple C–O bond cleavage in $\mathbf{1s}_{H^+}$ and $\mathbf{2s}_{H^+}$ to give the corresponding open-chain secondary and primary carbocations demonstrates that release of the H_2O molecule from these systems is anchimerically assisted by all the adjacent groups.

The preexponential factor for the hydride participation in $\mathbf{1s}_{H^+}$ (A_H) is five orders of magnitude lower than that for the competing phenyl-group participation (A_{Ph}). For $\mathbf{2s}_{H^+}$, A_H is six orders of magnitude lower than A_{Ph}, whereas the preexponential factor for the methyl-group participation (A_{Me}) is over four orders of magnitude lower than A_{Ph}. These large differences indicate that, under the experimental conditions used, neighboring-group assistance for unimolecular C–O bond fission in $\mathbf{1s}_{H^+}$ and $\mathbf{2s}_{H^+}$ is essentially governed by entropic, rather than enthalpic factors. Activation entropies for C–O bond cleavage in $\mathbf{1s}_{H^+}$ and $\mathbf{2s}_{H^+}$ cannot be associated exclusively with conformational equilibria or with statistical factors (two migrating β-hydrogens vs. a single phenyl group in $\mathbf{1s}_{H^+}$). Indeed, spectroscopic studies indicate that alcohols **1s** and **2s** in apolar solvents at room temperature preferentially acquire a gauche–anti conformation stabilized by intramolecular OH$\cdots\pi$-ring H-bonding.[22] This preference is further exalted in the isolated state and for the O-protonated derivatives $\mathbf{1s}_{H^+}$ and $\mathbf{2s}_{H^+}$.[22, 23] Scheme 7 shows the stability order of the rotamers of $\mathbf{1s}_{H^+}$ and $\mathbf{2s}_{H^+}$.

As a result, backside Ph participation in $\mathbf{1s}_{H^+}$ and $\mathbf{2s}_{H^+}$ would be the entropically least favored process, in contrast to its largest A_{Ph} experimental value. This excludes conformational factors as being the cause of the large $A_{Ph}/A_H = 10^5$–10^6 and $A_{Ph}/A_{Me} = 5 \times 10^4$ ratios of Table 9. The hypothesis of a low-energy low-entropy hydrogen migration in the collision complexes between $\mathbf{1s}_{H^+}$ or $\mathbf{2s}_{H^+}$ and an external $CH_3{}^{18}OH$ molecule is also unlikely, with the latter acting as a transducer of the migrating hydrogen moiety. Indeed, in this case, a pronounced loss of the deuterium label would be observable in the ***rac*-5** products from $\mathbf{1d}_{H^+}$ and $\mathbf{2d}_{H^+}$, in contrast with

0947-6539/99/0503-0842 $ 17.50+.50/0 *Chem. Eur. J.* **1999**, *5*, No. 3

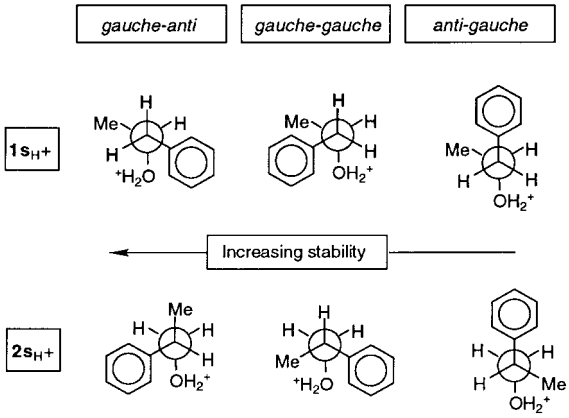

Scheme 7. Order of stability of the conformers of O-protonated (*S*)-1-phenyl-2-propanol and (*S*)-2-phenyl-1-propanol.

their high D retention (Table 4). Therefore, the large differences in the activation parameters of Table 9 can only be ascribed to the different position of the corresponding transition structures along the reaction coordinate. A comprehensive discussion of these aspects is reported in the following paper.

Inspection of Table 9 reveals that, in the gas phase, the activation energy for the backside $\mathbf{1s}_{H^+} \rightarrow \mathbf{Ir}$ ($E^{*\,back}_{Ph}$) is 1.3 ± 0.5 kcal mol^{-1} greater than that of the frontside $\mathbf{1s}_{H^+} \rightarrow \mathbf{Is}$ reaction ($E^{*\,front}_{Ph}$). Such a counterintuitive observation for the solution phase standards can be explained by considering that the process takes place in the absence of solvation and ion pairing. Indeed, while the experimental $E^{*\,front}_{Ph}$ concerns the $(\mathbf{1s}_{H^+})_{gauche} \rightarrow \mathbf{Is}$ step, the $E^{*\,back}_{Ph}$ refers to the overall $(\mathbf{1s}_{H^+})_{gauche} \rightarrow (\mathbf{1s}_{H^+})_{anti} \rightarrow \mathbf{Ir}$ sequence, in which the first step may cost several kilocaleries per mole.[24] Besides, the energy requirements for the gas-phase frontside $\mathbf{1s}_{H^+} \rightarrow \mathbf{Is}$ process may be mitigated by attractive electrostatic interactions in the transition structure between the leaving moiety H_2O and the phenyl ring of the cation. Similar electrostatic interactions are spatially prevented in the gas-phase backside $\mathbf{1s}_{H^+} \rightarrow \mathbf{Ir}$ process. This also explains the $A^{back}_{Ph}/A^{front}_{Ph} = \approx 50$ ratio in Table 9, which reflects the more restricted H_2O rotations and translations in the gas-phase frontside $\mathbf{1s}_{H^+} \rightarrow \mathbf{Is}$ process relative to the backside $\mathbf{1s}_{H^+} \rightarrow \mathbf{Ir}$ one. Of course, as pointed out in related gas-phase studies,[1] electrostatic interactions play only a minor role in solvolytic nucleophilic displacements owing to interference from the reaction medium (nucleophilicity, dielectric properties, etc.). In these media, conformational equilibria in ionic species can be strongly altered and electrostatic interactions between the nucleophile and the leaving moiety minimized, so that solvolysis is usually governed by stereoelectronic factors favoring backside participation.

Conclusions

a) The present gas phase results provide an experimental insight into vicinal-group anchimeric assistance in the unimolecular loss of H_2O from free O-protonated (*S*)-1-phenyl-2-propanol $\mathbf{1s}_{H^+}$ and (*S*)-2-phenyl-1-propanols $\mathbf{2s}_{H^+}$. Neighboring-group participation appears much less effective in promoting CH_3OH loss from free O-methylated (*S*)-1-phenyl-2-propanol $\mathbf{1s}_{Me^+}$ and (*S*)-2-phenyl-1-propanols $\mathbf{2s}_{Me^+}$.

b) Analysis of the activation parameters points to the neighboring-group assistance in $\mathbf{1s}_{H^+}$ and $\mathbf{2s}_{H^+}$ being regulated more by entropic than by enthalpic factors. Thus, at variance with previous indications,[11c] the more energy-demanding phenyl-group participation prevails over hydrogen participation under the conditions used only by virtue of its much less unfavorable activation entropy.

c) In $\mathbf{1s}_{H^+}$, competing phenyl-group (k_{Ph}) versus hydrogen (k_H) anchimeric assistance is observed. The same groups compete with methyl (k_{Me}) in anchimerically assisting C–O bond fission in $\mathbf{2s}_{H^+}$. The use of enatiomerically pure $\mathbf{1s}_{H^+}$ allowed us to discern between frontside (k^{front}_{Ph}) and backside phenyl-group participation (k^{back}_{Ph}).

d) The observation of frontside phenyl-group participation in $\mathbf{1s}_{H^+}$ (k^{front}_{Ph}), with an activation energy lower than that of the competing backside phenyl-group participation (k^{back}_{Ph}), is rationalized in terms of the favored gauche conformations in the chiral oxonium ion, and of the stabilizing interactions between the leaving H_2O and the ring of the phenonium ion.

e) In agreement with spectroscopic evidence in superacidic solutions[7] and in contrast with theoretical predictions,[25] phenyl-group participation in C–O bond cleavage in $\mathbf{1s}_{H^+}$ and $\mathbf{2s}_{H^+}$ gives rise to static, optically active 1,2-propenebenzenium intermediates that do not display any propensity for unimolecular ring opening and racemization through high-energy open-chain structures.

Acknowledgements

This research was supported by the Italian Ministero dell'Università e della Ricerca Scientifica e Tecnologica (MURST) and by the Italian National Research Council (CNR). We thank Anna Troiani for help with some of the early experimental work.

[1] a) D. J. Cram, *J. Am. Chem. Soc.* **1949**, *71*, 3863; b) D. J. Cram, R. Davis, *J. Am. Chem. Soc.* **1949**, *71*, 3875; c) D. J. Cram, *J. Am. Chem. Soc.* **1964**, *86*, 3767; d) S. Winstein, B. K. Morse, E. Grunwald, K. C. Schreiber, J. Corse, *J. Am. Chem. Soc.* **1952**, *74*, 1113.

[2] C. J. Lancelot, D. J. Cram, P. von R. Schleyer, *Carbonium Ions*, *Vol. III* (Eds.: G. A. Olah, P. von R. Schleyer) Wiley, New York, **1972**, chapter 27.

[3] a) H. C. Brown, *The Transition State*, *Special Publ. No. 16*, The Chemical Society, London, **1962**, p. 149; b) H. C. Brown, K. J. Morgan, F. J. Cloupek, *J. Am. Chem. Soc.* **1965**, *87*, 2137.

[4] a) H. C. Brown, R. Bernheimer, C. J. Kim, S. E. Scheppele, *J. Am. Chem. Soc.* **1967**, *89*, 370; b) H. C. Brown, C. J. Kim, *J. Am. Chem. Soc.* **1968**, *90*, 2080; c) W. H. Saunders, Jr., S. Asperger, D. H. Edison, *J. Am. Chem. Soc.* **1958**, *80*, 2421; d) S. L. Loukas, M. R. Velkou, G. A. Gregoriou, *J. Chem. Soc. Chem. Commun.* **1969**, 1199; e) S. L. Loukas, F. S. Varveri, M. R. Velkou, G. A. Gregoriou, *Tetrahedron Lett.* **1971**, 1803.

[5] B. Capon, S. P. McManus, *Neighboring Group Participation*, *Vol. 1*, Plenum, New York, **1976**.

[6] a) G. A. Olah, R. D. Porter, *J. Am. Chem. Soc.* **1970**, *92*, 7627; b) G. A. Olah, R. D. Porter, *J. Am. Chem. Soc.* **1971**, *93*, 6877; c) G. A. Olah, R. J. Spear, D. A. Forsyth, *J. Am. Chem. Soc.* **1976**, *98*, 6284.

[7] G. A. Olah, N. J. Head, G. Rasul, G. K. Surya Prakash, *J. Am. Chem. Soc.* **1995**, *117*, 875 (see also: S. Sieber, P. von R. Schleyer, J. Gauss, *J. Am. Chem. Soc.* **1993**, *115*, 6987).

[8] G. A. Olah, R. J. Spear, D. A. Forsyth, *J. Am. Chem. Soc.* **1977**, *99*, 2615.
[9] a) W. J. Hehre, *J. Am. Chem. Soc.* **1972**, *94*, 5919; b) S. Yamabe, T. Tanaka, *Nippon Kagaku Kaishi* **1986**, *11*, 1388. See also ref. [6c].
[10] a) T. H. Morton, *Tetrahedron* **1982**, *38*, 3195; b) D. J. McAdoo, T. H. Morton, *Acc. Chem. Res.* **1993**, *26*, 295.
[11] a) S. Fornarini, C. Sparapani, M. Speranza, *J. Am. Chem. Soc.* **1988**, *110*, 34; b) S. Fornarini, C. Sparapani, M. Speranza, *J. Am. Chem. Soc.* **1988**, *110*, 42; c) S. Fornarini, V. Muraglia, *J. Am. Chem. Soc.* **1989**, *111*, 873.
[12] a) C. Koppel, C. C. van der Sande, N. M. M. Nibbering, T. Nishishita, F. W. McLafferty, *J. Am. Chem. Soc.* **1977**, *99*, 2883; b) C. N. McEwen, M. A. Rudat, *J. Am. Chem. Soc.* **1981**, *103*, 4355; c) M. Carsten, D. Kuck, *Org. Mass Spectrom.* **1993**, *28*, 1073; d) W. Bäther, H. F. Grützmacher, *Int. J. Mass Spectrom. Ion Proc.* **1985**, *64*, 193: e) D. Kuck, *Mass Spectrom. Rev.* **1990**, *9*, 583.
[13] a) F. Cacace, *Acc. Chem. Res.* **1988**, *21*, 215; b) M. Speranza, *Mass Spectrom. Rev.* **1992**, *11*, 73.
[14] H. C. Brown, G. Zweifel, *J. Am. Chem. Soc.* **1960**, *82*, 4708.
[15] D. Achet, D. Rocrelle, I. Murengezi, M. Delmas, A. Gaset, *Synthesis* **1986**, 643.
[16] $G(C_nH_5^+(n=1,2)) = 2.8$: a) P. Ausloos, S. G. Lias, R. Gorden, Jr., *J. Chem. Phys.* **1963**, *39*, 3341; b) P. Ausloos, *Ion-Molecule Reactions* (Ed.: J. L. Franklin), Plenum, New York, **1970**; c) P. Ausloos, S. G. Lias, *J. Chem. Phys.* **1962**, *36*, 3163; d) S. G. Lias, P. Ausloos, *J. Chem. Phys.* **1962**, *37*, 877.
[17] The irradiated systems invariably contain $H_2{}^{16}O$, as ubiquitous impurity, either initially introduced in the mixture together with its bulk component or formed from its radiolysis. As pointed out previously (A. Troiani, F. Gasparrini, F. Grandinetti, M. Speranza, *J. Am. Chem. Soc.* **1997**, *119*, 4525; M. Speranza, A. Troiani, *J. Org. Chem.* **1998**, *63*, 1020.), the average stationary concentration of $H_2{}^{16}O$ in the radiolytic systems is estimated to approach that of the added $H_2{}^{18}O$ (ca. 2–3 Torr). Therefore, the $\leq 40\%$ ^{18}O incorporation in **1s** is interpreted in terms of the intermolecular **2s** → **1s** isomerization mechanism, shown in path ii) → iii) of Scheme 4.
[18] The binding energy in the cluster between *tert*-butyl cation and water is estimated as large as about 11 kcal mol^{-1} by high-level ab initio calculations (D. Berthomieu, H. E. Audier, *Eur. Mass Spectrom.* **1997**, *3*, 19). The interaction energy in electrostatically bonded clusters between carbocations and *n*-type donors is rather insensitive of the nature of both the ion and the donor, whether H_2O or CH_3OH (see, for instance: a) M. Meot-Ner (Mautner), Z. Karpas, C. Deakyne, *J. Am. Chem. Soc.* **1986**, *108*, 3913; b) H. E. Audier, G. K. Koyanagi, T. B. McMahon, D. Thölmann, *J. Phys. Chem.* **1996**, *100*, 8220; c) E. Uggerud, *J. Am. Chem. Soc.* **1994**, *116*, 6873; d) M. Meot-Ner (Mautner), M. M. Ross, J. E. Campana, *J. Am. Chem. Soc.* **1985**, *107*, 4839).
[19] In the absence of NMe_3, neutralization of the O-protonated ethers, arising from addition of **Ir**, **IVr**, and **IVs** to methanol, may proceed through several pathways, including proton transfer to the substrate itself, to the walls of the reaction vessel, or to adventitious bases, either initially added to the gaseous mixture or formed from its radiolysis.
[20] This extension is valid only if the secondary kinetic β-deuterium effects on the phenyl and methyl-group participation in $\mathbf{2s}_{H^+}$ are taken equal to unity. The validity of this assumption is demonstrated in the following paper.
[21] The reaction time is taken as the inverse of the pseudo first-order collision rate constant $k = k_{coll}[CH_3{}^{18}OH]$ between $\mathbf{1s}_{H^+}$ (or $\mathbf{2s}_{H^+}$) and the $CH_3{}^{18}OH$ nucleophile, with the collision rate constant k_{coll} calculated according to T. Su, W. J. Chesnavitch, *J. Chem. Phys.* **1982**, *76*, 5183; [k_{coll} ($\times 10^9$ cm^3 molecule^{-1} s^{-1}) = 1.81 (25 °C); 1.74 (60 °C); 1.70 (85 °C); 1.67 (100 °C); 1.64 (120 °C); 1.62 (140 °C)].
[22] a) M. J. Cook, T. A. Khan, K. Nasri, *Tetrahedron Lett.* **1984**, 5129; b) M. J. Cook, T. A. Khan, K. Nasri, *Tetrahedron* **1986**, *42*, 249.
[23] J. J. Urban, C. W. Cronin, R. R. Roberts, G. R. Famini, *J. Am. Chem. Soc.* **1997**, *119*, 12292.
[24] S. Usui, M. Okamura, A. Ohno, *Proceedings of the VII Kyushu International Symposium on Physical Organic Chemistry*, Kyushu University, December 2–5, **1997**.
[25] H. Griengl, P. Schuster, *Tetrahedron* **1974**, *30*, 117.

Received: June 16, 1998 [F1211]

0947-6539/99/0503-0844 $ 17.50+.50/0 *Chem. Eur. J.* **1999**, *5*, No. 3